ADVANCED MATERIALS

Supporting Information

for *Adv. Mater.*, DOI: 10.1002/adma.201700628

Reprogrammable Phononic Metasurfaces

Osama R. Bilal, André Foehr, and Chiara Daraio**

DOI: 10.1002/adma.201700628R2

Supporting Information

Reprogrammable phononic metamaterial plates

Osama R. Bilal, André Foehr & Chiara Daraio**

Magnetic potential and material programming We characterize the magnetic force between a 3×3 array of magnets of diameter 5 mm and thickness of 4 mm resembling the controllable magnetic field underneath the metamaterial plate. We fix the array to the force-sensing clamp in the Instron 3000 mechanical testing machine. We fix another array of 3×3 magnets to the opposite Instron clamp, 3 mm diameter and 2 mm thickness similar to the magnets embedded in the metamaterial. We start the compression test with the magnets at 15 mm distance. We move the magnet arrays close to each other and record the repulsion force in **Figure S1a**. We divide the measured data by 9, to obtain the interaction force of each individual pair of repelling magnets, assuming no interactions between the adjacent magnets in the array.

The experimentally measured magnetic force is represented by the following equation as a function of displacement, x:

$$\mathrm{f_{Mag}} = 1.6467\exp^{-450.8\left(x+x_0(t)\right)} + 1.2378\mathrm{e}-3,$$

where the time dependent position of the control magnet is denoted as $x_0(t)$. This function is then incorporated into the equation of motion for the system to obtain both **Figure 2a and b**:

$$m\ddot{x} = -d\dot{x} - kx + f_{Mag}$$

We use the fitted force equation to setup a finite element stationary analysis using COMSOL software. The resulting shapes of the different applied force on the unit cells (flat and deflected) are included in the inset in **Figure S1b**. These shapes agree with the experimentally

obtained unit cell deflections in **Figure 1a-b**. The obtained force-distance curve (**Figure S1a**) shows a nonlinear continuous increase in the force amplitude, as the distance between the plate and the magnetic stage decreases.

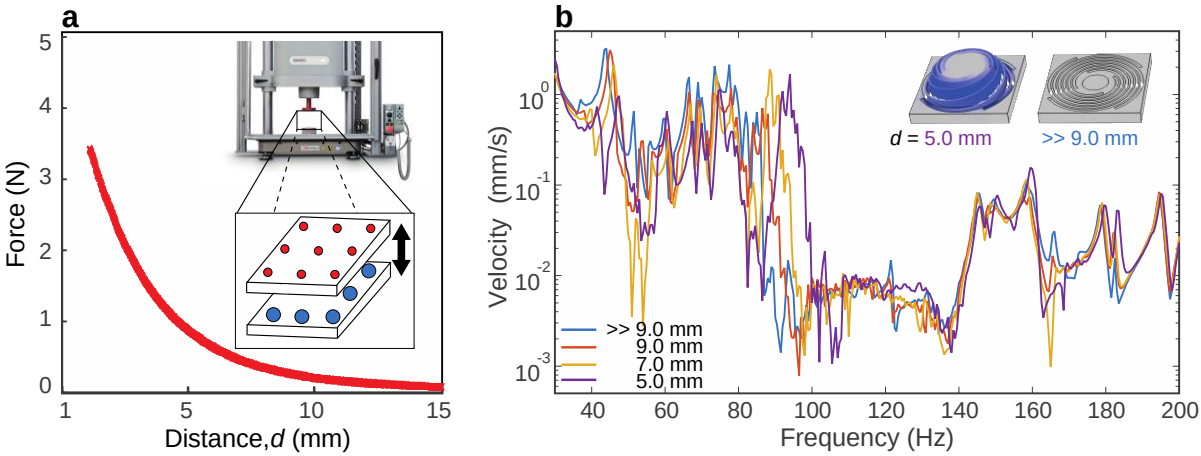

Figure S1. (a) The measured repulsion forces between control magnets, placed underneath the metamaterial, and the embedded magnets in the center of each metamaterial unit cell. The inset shows a schematic diagram of the experimental setup, where red and blue are the positive and negative polarizations of the magnets. (b) Particle velocity measured at the center of a spiral unit cell, with various magnetic potentials (with the moving magnetic stage at different distances, d, from the plate). The inset shows both the flat and programmed unit cells.

To characterize the influence of the tuning distance on the wave propagation within the plate, we excite the plate harmonically and record its response at various tuning distances. The measured wave velocity, at different frequencies for four stage positions, are plotted in **Figure S1b**. The magnetic repulsion forces between the stage magnets and the ones at the center of each unit cell correlate with the added stiffness to the mode shape at the edge of the band gap. Therefore, as the distance between the plate and the stage decreases, the frequency of the band gap edge increases. Due to the continuity of the force-distance curve, the material can be programmed in either a binary or an analog fashion. To achieve binary programming of the material (i.e., 0 or 1), we set the magnetic stage to only stop at two predetermined positions (z_1 and z_2) along the z-direction. The positions are chosen such that maximum difference in transmission amplitude is present, as indicated by the dashed line in **Figure 2c**. Analog

programming, on the other hand, could be achieved by allowing the stage to stop at any position between z_1 and z_2, as presented in **Figure 1e**.

Band structure analysis for the metamaterial We evaluate the metamaterial band structure using the finite element method. We model an infinite array of the spiral unit cells in both x and y directions. We solve the elastic wave equations for a heterogeneous medium [*1*]:

$$\nabla . C : \frac{1}{2}(\nabla u + (u)^T) = \rho \ddot{u}, \quad (1)$$

where ∇ is the gradient operator, C is the elasticity tensor, u is the displacement vector, ρ is the density, and $(.)^T$ is the transpose operation. To obtain the band structure we apply the Bloch wave formulation in both *x* and y directions (i.e., Bloch boundary conditions).[S2] The Bloch solution is assumed to be in the form $u(x, k;\ t) = \tilde{u}(x, k)e^{i(k.x-\omega t)}$ where $\tilde{u}$ is the Bloch displacement vector, $x = \{x, y, z\}$ is the position vector, k is the wave vector, ω is the frequency, and t is the time. We consider the wave propagation along the edges of the irreducible Brillouin zone, in the Γ−X−M−Γ directions (**Figure S2a**). The region of no transmission (band gap) is shaded in gray. We compare the theoretically obtained dispersion curves in **Figure S2a**, to the experimentally measured transmission signal at the center of the fabricated finite metamaterial plate, consisting of an array of 28×20 unit cells. We fix the corners of the metamaterial array and excite the top center of the plate. We obtain the frequency response function of the metamaterial in **Figure S2b**. Both finite and infinite predictions agree well, particularly in the band gap frequency range, highlighted in gray. Outside of this gray area, there exist frequency regions with low transmission. However, these regions are not full band gaps (i.e., a band gap for all mode shapes, along all symmetry directions). In our dispersion analysis, we use a full 3D finite element modeling, to capture all aspects of the unit cell dispersion. What we refer to as a band gap is a complete band gap. However, there are bands within the dispersion curves that correspond to pure out-of-plane modes or in-plane modes. If we only excite the plate out-of-plane, which is the case in our

experiments, these branches (modes) are not excited and therefore would correspond to lower transmission regions within the FRF diagrams.

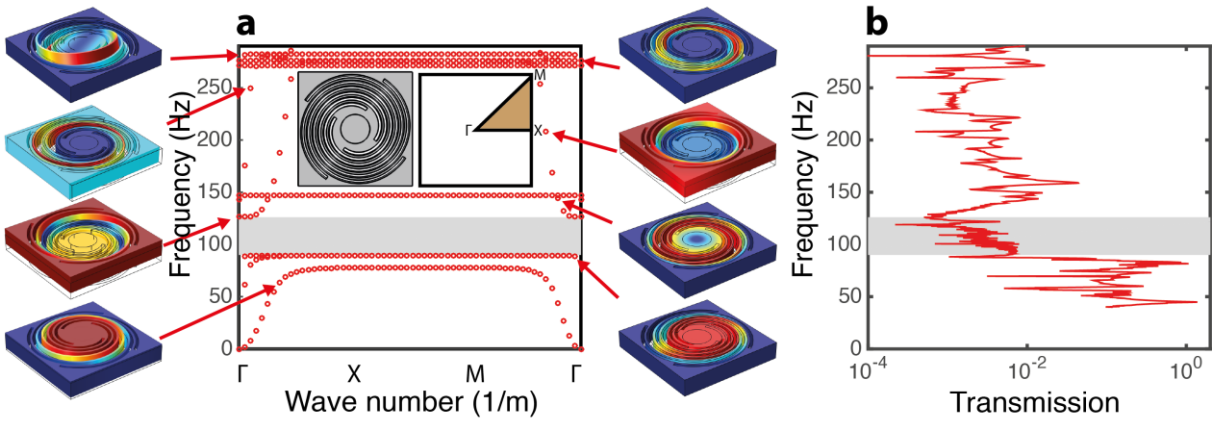

Figure S2. Theory Vs. Experiments: theoretical dispersion curves with unit cell design and its corresponding irreducible Brillouin zone in the inset. Experimental response of the system with an excellent agreement in comparison to the theory particularly within the band gap region, highlighted in gray. Different mode shapes are plotted with an arrow indicating the frequency of each mode.

Metamaterial quality factor We characterize the quality factor, *Q*, of the spiral-spring resonators in the metamaterial by measuring the resonance amplitude of a single spring using a mechanical shaker as a harmonic excitation source and a laser Doppler vibrometer to detect the velocity of the central mass of the spring. The calculated $Q = f/\Delta f \; is \approx 52$ (**Figure S3**), where f is the resonance frequency and Δf is the width of the frequency range for which the amplitude is $1/\sqrt{2}$ of its peak value.

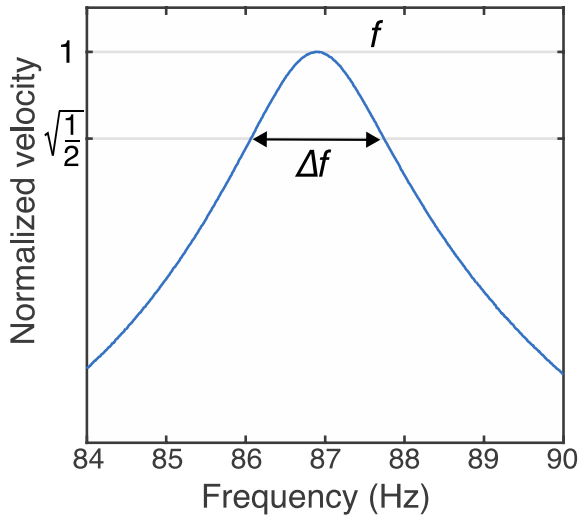

Figure S3. Experimental characterization of a single spiral-spring resonator made out of polycarbonate.

Supplementary movie 1 The movie shows the metamaterial in the flat 2D configuration and how it transforms to the programmed 3D state creating the ETH logo. The metamaterial is then transformed back to the 2D state. All in real-time.

References

[S1] Osama R. Bilal and Mahmoud I. Hussein, Ultrawide phononic band gap for combined in-plane and out-of-plane waves, Phys. Rev. E. (R) 84, 2011

[S2] Léon Brillouin, Wave propagation in periodic structures: electric filters and crystal lattices. Dover Books, 1946.